Northumbria Research Link

Citation: Sun, Jiahao, Lin, Qiu, Liu, Xing, Ma, Jien, Fang, Youtong and Wu, Haimeng (2021) Dynamic Control of Three-Phase Dual-Active-Bridge DC-DC Converters Based on Sliding-Mode-Learning Adaline. In: 2021 IEEE 1st International Power Electronics and Application Symposium (PEAS). IEEE, Piscataway, US, p. 9628778. ISBN 9781665413619, 9781665413596, 9781665413602

Published by: IEEE

URL: https://doi.org/10.1109/PEAS53589.2021.9628778 <https://doi.org/10.1109/PEAS53589.2021.9628778>

This version was downloaded from Northumbria Research Link: http://nrl.northumbria.ac.uk/id/eprint/47249/

Northumbria University has developed Northumbria Research Link (NRL) to enable users to access the University's research output. Copyright © and moral rights for items on NRL are retained by the individual author(s) and/or other copyright owners. Single copies of full items can be reproduced, displayed or performed, and given to third parties in any format or medium for personal research or study, educational, or not-for-profit purposes without prior permission or charge, provided the authors, title and full bibliographic details are given, as well as a hyperlink and/or URL to the original metadata page. The content must not be changed in any way. Full items must not be sold commercially in any format or medium without formal permission of the copyright holder. The full policy is available online: http://nrl.northumbria.ac.uk/policies.html

This document may differ from the final, published version of the research and has been made available online in accordance with publisher policies. To read and/or cite from the published version of the research, please visit the publisher's website (a subscription may be required.)

Northumbria University NEWCASTLE

University Library

Dynamic Control of Three-Phase Dual-Active-Bridge DC-DC Converters Based on Sliding-Mode-Learning Adaline

1st Jiahao Sun
College of Electrical Engineering
Zhejiang University
Hangzhou, China
11810062@zju.edu.cn

2nd Lin Qiu
College of Electrical Engineering
Zhejiang University
Hangzhou, China
qiu_lin@zju.edu.cn

3rd Xing Liu
College of Electrical Engineering
Zhejiang University
Hangzhou, China
xingldl@zju.edu.cn

4th Jien Ma
College of Electrical Engineering
Zhejiang University
Hangzhou, China
majien@zju.edu.cn

5th Youtong Fang
College of Electrical Engineering
Zhejiang University
Hangzhou, China
youtong@zju.edu.cn

6th Haimeng Wu
Department of Mathematics, Physics and Electrical Engineering
Northumbria University
Newcastle, UK
Haimeng.wu@northumbria.ac.uk

***Abstract*—Fast dynamic response is an important requirement for three-phase dual active bridge (3p-DAB) DC-DC converters under the varied source voltage and load resistance conditions. In order to enhance the dynamic performance of output voltage of 3p-DAB, a novel nonlinear controller, which is combined with the proportional plus derivative (PD) controller and the adaptive linear element (Adaline), is proposed in this paper. Firstly, a sliding-mode-learning strategy is presented for the Adaline to improve the robustness of adaptive learning. Meanwhile, the output of the Adaline is added to the output of PD controller for ensuring an outstanding dynamic response of output voltage with less overshoot. Furthermore, a comparison with the PI controller based on phase shift modulation is implemented by simulation tool to validate the utility and effectiveness of the proposed control scheme. Finally, experimental comparison results on a laboratory prototype are presented to further verify the theoretic analysis and the effectiveness of the proposed control method.**

***Index Terms*—Adaptive linear element (Adaline), three-phase dual active bridge (3p-DAB), sliding-mode-learning, voltage regulation**

I. Introduction

With the aggravation of the impact of greenhouse gas emissions on the environment, the reduction of carbon dioxide emission is obtained increasing attention in public. For this purpose, more and more countries put more attention on the electrification evolution. Subsequently, large scales of renewable energy generation and distribution storage systems are utilized in the medium-voltage electrical distribution grids. Bidirectional DC-DC converters are the key components for these applications. They play as the interface between the energy sources and the DC micro-girds [1], which requires the capacity of power flow between different bus voltage levels with high efficiency and the voltage/current regulation with fast response [2].

Among various scenarios, the dual-active-bridge (DAB) DC-DC converter is a prominent choice due to the soft-switching capacity, few passive components required and high power density [3]–[5]. Compared with the single DAB, the three-phase DAB (3p-DAB) has some outstanding advantages, such as the better utilization of magnetic material of the high-frequency transformer and the smaller dc-link capacitors for the filter [6], [7]. Therefore, it attracts more and more interests from researchers. The application of DC micro-grids demands that the interface converter can ensure the fast dynamic response for the load disturbance and the voltage regulation. In order to meet the requirements, numerous control strategies are proposed for the DAB and 3p-DAB topologies. In [8], a closed-loop PI controller based on the generalized average modeling technique is proposed to improve the dynamic performance of DAB. However, due to the limitation of the designed equilibrium point, the performance will be deteriorated when the desired operation point is far away from the designed equilibrium point. In [9], an adaptive dynamic control based on a novel harmonic modeling strategy is proposed, which adds a feed-forward to compensate the disturbance. However, a look-up table is utilized in this method that will occupy the RAM of micro-processor. Accordingly, it prevents further application in practice. In [10], an improved model-based phase-shift control for DAB is proposed to enhance the dynamic performance. Nevertheless, the uncertainties or disturbance of the system will impact the performance of the control scheme. In [11], [12], an instantaneous current control is proposed for 3p-DAB to improve the dynamic response of system, which can control the transformer current to steady state in one-third of a

switching period. From the aforementioned research works, it can be found that most of the control scheme is based on the linear controller with some compensations. But the dynamic performance of these control strategies will be deteriorated, when the application is operated in the wide load range.

In order to address this issue, a novel nonlinear controller, which is combined with the proportional plus derivative (PD) controller and the adaptive linear element (Adaline), is proposed in this paper. First of all, a sliding-mode-learning algorithm (SMLA) is presented for the training of weight vector of the Adaline to enhance the robustness of adaptive learning. Meanwhile, the output of the Adaline is added to the output of PD controller for ensuring an outstanding dynamic response of output voltage with less overshoot. Moreover, the performance of the proposed control algorithm is verified with different simulations on a 1kW 3p-DAB converter, and a PI control scheme based on phase shift modulation (PSM) is also test for comparison. Finally, the experimental comparison results are provided to confirm the theoretical analysis and the effectiveness of the proposed solution.

The rest of this paper is organized as follows: Section II introduces the structure and the principle of PSM for 3p-DAB. In Section III, The principle and the design of the proposed control scheme is described in detail. Thereafter, the comparison simulation results and the comparison experimental results are provided in Section IV to validate the improvement of the dynamic performance of the proposed nonlinear controller for 3p-DAB. Finally, the conclusion is summarized in Section V.

II. Principle of the 3p-DAB under PSM

A. Introduction of 3p-DAB

The schematic diagram of 3p-DAB DC-DC converter is given in Fig. 1, where two three-phase active bridges are connected by a three-phase high-frequency transformer with turn ratio $N:1$. $L_{si}(i=a,b,c)$ is the leakage inductance. The transformer equivalent series resistance and the core losses are neglected in this paper, and the leakage inductance of each phase is assumed equal for simplifying the next analysis. C_i and C_o are the filter capacitors of input port and output port, respectively. They can be utilized to reduce the voltage ripple. R_L is the load resistor.

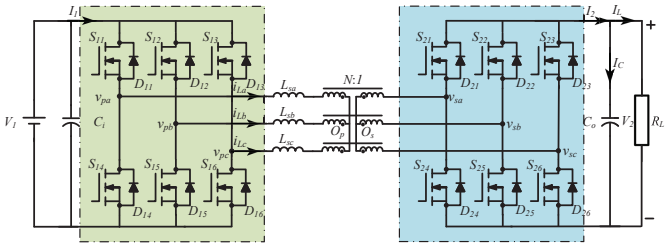

Fig. 1. Schematic diagram of the 3p-DAB.

B. Introduction of PSM for the 3p-DAB

The PSM is the common modulation strategy for 3p-DAB due to its inherent zero-voltage switching capability and ease of implementation [13]. In order not to lose generality, a forward power-flow case is analyzed here, whereas the same method is also applicable to the backward case. For the PSM, the outer phase shift ratio D_ϕ with respect to half of switching period T_{hs} is the only control variable. $D_\phi T_{hs}$ is the phase shift angle between the two three-phase active bridges, and its range is $[0,\frac{1}{2}]$. The square waves of each phase are phase shifted to each other by $\frac{\pi}{3}$. Therefore, only one phase needs to be analyzed. According to the characteristics of PSM, the key steady state waveforms of PSM can be divided into two case: (a) $0<D_\phi\le\frac{1}{3}$, (b) $\frac{1}{3}<D_\phi\le\frac{1}{2}$, which are shown in Fig. 2. It can be observed that each three-phase bridge produces a six-step mode square voltage with discrete voltage levels, i.e. $\pm\frac{V_1}{3}$ and $\pm\frac{2V_1}{3}$ for primary bridge, and $\pm\frac{V_2}{3}$ and $\pm\frac{2V_2}{3}$ for secondary bridge. The related transferred power of each case can be expressed as [14]:

$$P_t=\begin{cases}\dfrac{NV_1V_2D_\phi}{f_sL_s}\left(\dfrac{1}{3}-\dfrac{D_\phi}{4}\right),\left(0\le D_\phi\le\dfrac{1}{3}\right)\\ \dfrac{NV_1V_2}{f_sL_s}\left(\dfrac{D_\phi}{2}-\dfrac{D_\phi^2}{2}-\dfrac{1}{36}\right),\left(\dfrac{1}{3}<D_\phi\le\dfrac{1}{2}\right)\end{cases}\tag{1}$$

where $f_s=1/2T_{hs}$ is the switching frequency.

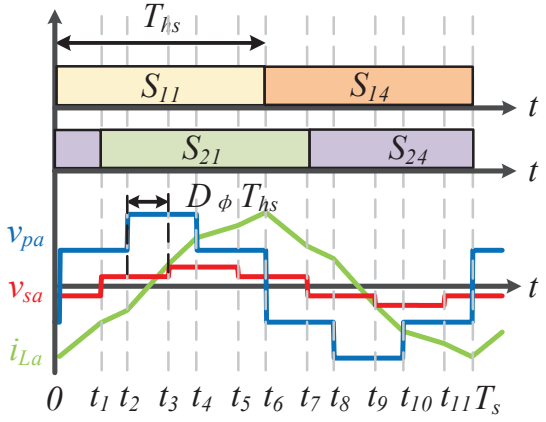

(a)

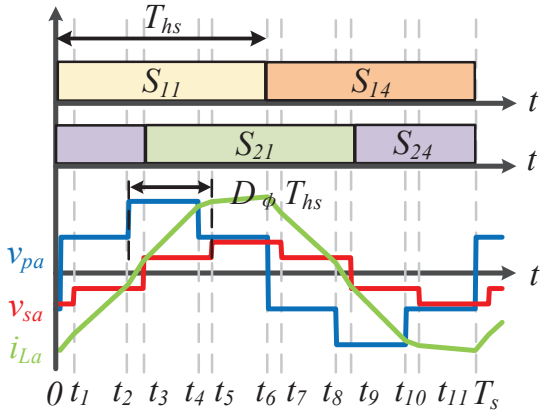

(b)

Fig. 2. Steady state operation of the 3p-DAB under PSM. (a) $0<D_\phi\le\frac{1}{3}$. (b) $\frac{1}{3}<D_\phi\le\frac{1}{2}$.

III. Principle of the Proposed Controller

According to the above discussion, it can be learned that there exists monotonicity between the P_t and D_ϕ, and the desired D_ϕ can be obtained by solve the equation (1). However, the variance of the system parameters and the load disturbances in practice implementation will affect the accuracy of the desired D_ϕ and the dynamic performance. Hence, this paper proposes a novel nonlinear controller that combined the PD controller and the Adaline to solve the above issues.

A. Introduction of the Adaline based on the sliding-mode-learning

First of all, the structure diagram of the Adaline is depicted in Fig. 3, where $x(t) = [x_1(t), x_2(t)...x_n(t), b]^T$ denotes the time-varying input vector, and $w(t) = [w_1(t), w_2(t)...w_n(t), w_{n+1}(t)]^T$ represents the weighting vector. The boundaries of these vectors can be defined as follows.

$$\| x(t) \| = \sqrt{x_1^2(t) + x_2^2(t) + ... + x_n^2(t) + b^2} \leq V_x \forall t \quad (2)$$

$$\| \dot{x}(t) \| = \sqrt{\dot{x}_1^2(t) + \dot{x}_2^2(t) + ... + \dot{x}_n^2(t)} \leq V_x \forall t \quad (3)$$

$$\| w(t) \| = \sqrt{w_1^2(t) + w_2^2(t) + ... + w_n^2(t) + w_{n+1}^2} \leq V_w \forall t. \quad (4)$$

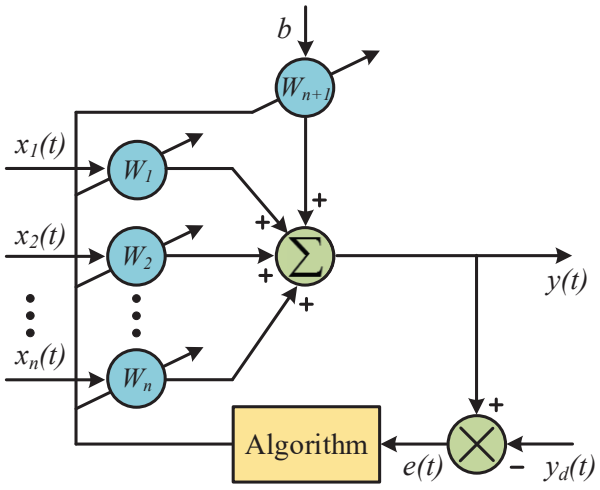

Fig. 3. Structure diagram of the Adaline.

In Fig. 3, the scalar signals $y_d(t)$ and $y(t)$ are the time-varying desired output and the actual output of the Adaline, respectively. We assume that $y_d(t)$ and $y(t)$ are bounded signals, and their boundaries condition can be described as follows.

$$\begin{aligned} |y_d(t)| &\leq V_y \forall t \\ |\dot{y}_d(t)| &\leq V_{\dot{y}} \forall t. \end{aligned} \quad (5)$$

Then, the expression of $y(t)$ can be obtained as:

$$y(t) = w^T x = \sum_{i=1}^{n} w_i(t) x_i(t) + w_{n+1} b \quad (6)$$

where b is a constant positive input, which can affect the threshold weight $w_{n+1}(t)$ in the Adaline.

Finally, the definition of the learning error $e(t)$ is presented as follows.

$$e(t) = y_d(t) - y(t). \quad (7)$$

B. Principle of the proposed controller combined with PD controller and the adaptive Adaline

The control diagram of the proposed nonlinear controller is presented in Fig. 4. In this paper, an SMLA is proposed to train the weighting vector of Adaline. In order to eliminate the voltage tracking error, two sliding surfaces are needed to be designed. One is the sliding surface s_a of the weighting vector training, the other is sliding surface s_c of the system control. The s_a can be designed as follows.

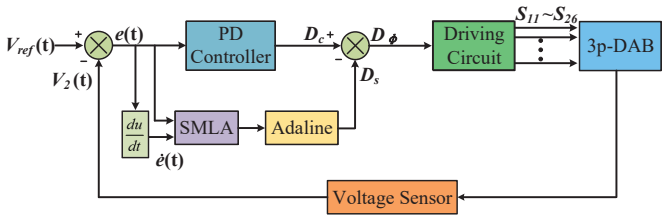

Fig. 4. Control diagram of the proposed nonlinear controller.

$$s_a = D_s + D_\phi = D_c = 0 \quad (8)$$

where

$$D_c = K_p e + K_d \dot{e} \quad (9)$$

$$D_s = w^T x \quad (10)$$

where K_p is the proportional gain, and K_d is the derivative gain.

The adaptation law based on SMLA for the weighting vector training can be designed as

$$\dot{w} = -(\frac{x}{x_T x}) k sign(s_a) \quad (11)$$

where $e = [e, \dot{e}, b]^T$ and $w = [w_1, w_2, w_3]^T$. The expression of signum function is defined in (11), and the coefficient k should satisfy the inequality (12).

$$sign(s_a) = \begin{cases} 1, & for\ s_a > 0 \\ 0, & for\ s_a = 0 \\ -1, & for\ s_a < 0 \end{cases} \quad (12)$$

$$k \geq V_w^T V_x + V_{\dot{y}} + \eta \quad (13)$$

where η is designed as positive constant.

In order to reduce the impact of the chatting, a saturation function is designed to replace the signum function, the designed saturation function is given by

$$sat(s_a) = \begin{cases} sign(s_a), & for\ |s_a| > \Delta \\ \frac{s_a}{\Delta}, & for\ |s_a| \leq \Delta \end{cases} \quad (14)$$

where Δ is the width of the boundary. In this paper, Δ is set as 0.02;

The sliding surface s_a can ensure the voltage tracking error converged to zero in finite time, and its design can be written as:

$$s_c = ae + \dot{e} = 0. \tag{15}$$

Let the coefficient $a = K_p/K_d$. Then, the sliding surface s_c will directly relate to the sliding surface s_a, and their relationship can be obtained as:

$$s_c = \frac{K_p}{K_d}e + \dot{e} = \frac{D_c}{K_d} = \frac{s_a}{K_d}. \tag{16}$$

Hence, the designed sliding surfaces s_a and s_c can simultaneously reach the designed sliding planes in finite time.

IV. Simulation And Experimental Results

To validate the effectiveness and superiority of the proposed control scheme, the simulation and the experimental comparison results are given in this section. The simulations are implemented with PLECS toolbox for MATLAB. The specifications and system parameters of the 3p-DAB prototype are listed in Table I. To outstand the dynamic performance of the proposed scheme, the reference output voltage variance and the constant power load (CPL) conditions are also considered. In order to highlight the dynamic performance of the proposed control strategy, comparative studies between the proposed control scheme and the PI control based on PSM are given in this section. The PI controller is designed based on the ideal math model under the equilibrium point $100V/80V$ 320W. The design method of the PI controller is depicted in [15].

TABLE I
System and Control Parameters of the Prototype

Parameter	Value
Input DC voltage (V_1)	100V
Output DC voltage (V_2)	$60 \sim 120$V
Transformer turn ratio (N)	$1:1$
Switching frequency (f_s)	20kHz
Equivalent series inductance (L_s)	27μH
Input DC capacitor (C_i)	200μF
Output DC capacitor (C_o)	200μF
Proportional coefficient (K_p)	0.05
Derivative coefficient (K_d)	0.001
The coefficient of SMLA (k)	600
Proportional coefficient (k_p)	0.03
Integral coefficient (k_i)	46.6
Rated power	1kW

A. Simulation results

First of all, Fig. 5 displays the simulation comparison results when the reference output voltage steps from 60V to 80V at time 0.1s. The load resistance is set as 20Ω. From the results, it can be observed that the overshoot voltage of the proposed control strategy is less than that of PI control, and the settle time of the proposed control strategy is also less than that of PI control. Next, the CPL is tested, and the desired transmission power is 180W, and the reference output voltage is 60V. In the practice application, the point-of-load (POL) converters are referred to as CPL. In this paper, we use the buck converter to simulate the CPL. The comparison results are presented in Fig. 6. It can be found that the dynamic performance of the proposed control strategy is better than PI control, which verifies the effectiveness and the salient performance of the proposed control strategy.

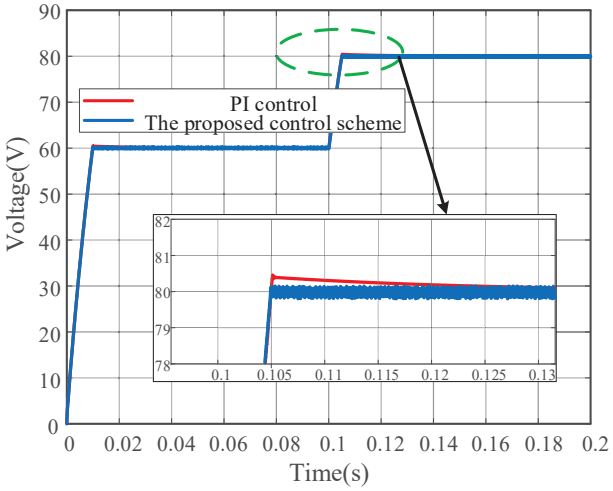

Fig. 5. Comparison results for the step of the reference output voltage.

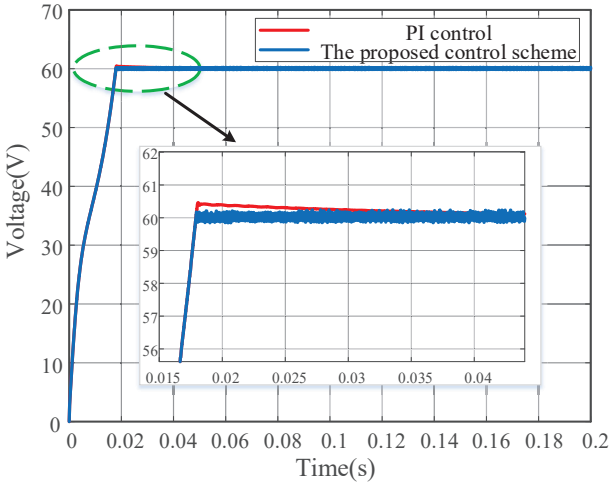

Fig. 6. Comparison results for the constant power load.

Finally, the load disturbance rejection ability is validated by measuring the output impedance. In order to evaluate the output impedance of the 3p-DAB, the perturbation AC current is injected to load. The output impedance evaluation circuit diagram is given in Fig. 7, which is implemented by the Simulink software. The 3p-DAB can be equivalent to a voltage source V_{out} and an output impedance Z_{out}. The steady-state load current I_L is set as the equilibrium point. i_{ac} represents the small-signal perturbation. The output voltage

V_2 is measured at each frequency of i_{ac}. Hence, the output impedance Z_{out} can be expressed as:

$$Z_{out}(f) = \frac{V_2(f)}{i_{ac}(f)}. \tag{17}$$

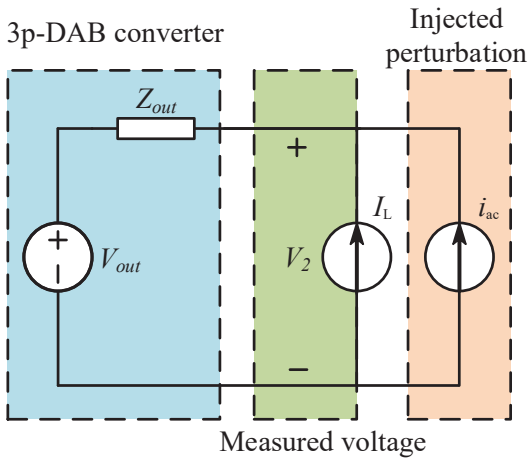

Fig. 7. Evaluation circuit of output impedance.

The comparison result of output impedance is shown in Fig. 8. It is easy to found that the proposed control scheme can keep low output impedance for the 3p-DAB in a wide frequency range, which demonstrates that the proposed control strategy has strong load current disturbance rejection ability.

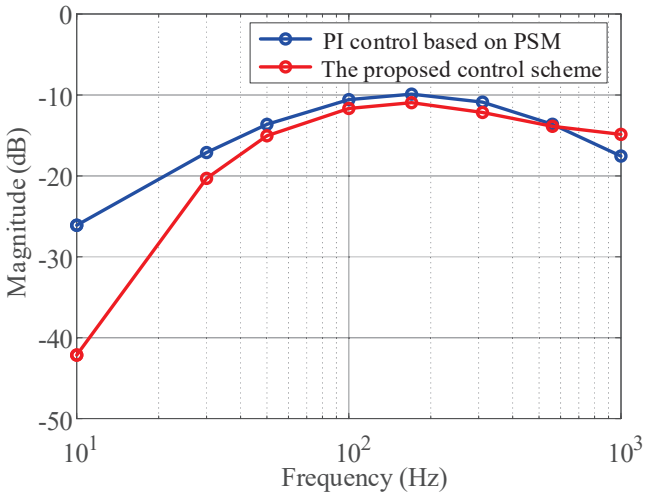

Fig. 8. Output impedance comparison results for PI control based on PSM and the proposed control scheme.

B. Experiment results

To demonstrate the theoretical analysis of the proposed solution and the above simulation comparison results, comparative experiments with PI control based on PSM are conducted in a prototype of the 3p-DAB converter. The photograph of the experimental setup is presented in Fig. 9. A DSP evaluation board is employed to implement the proposed control strategy. The output voltage is sampled by the LV-25P.

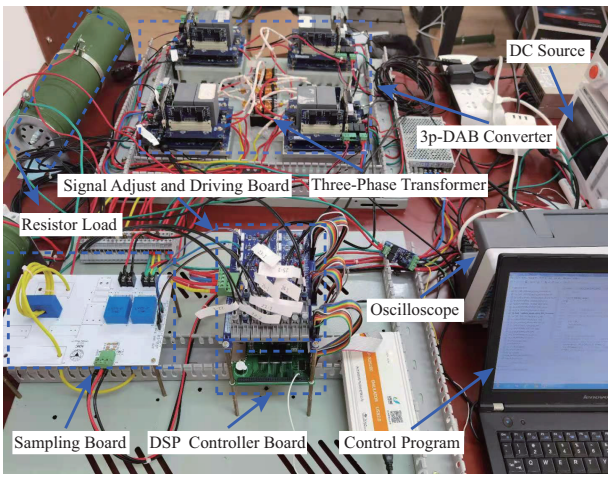

Fig. 9. Photograph of the experimental setup.

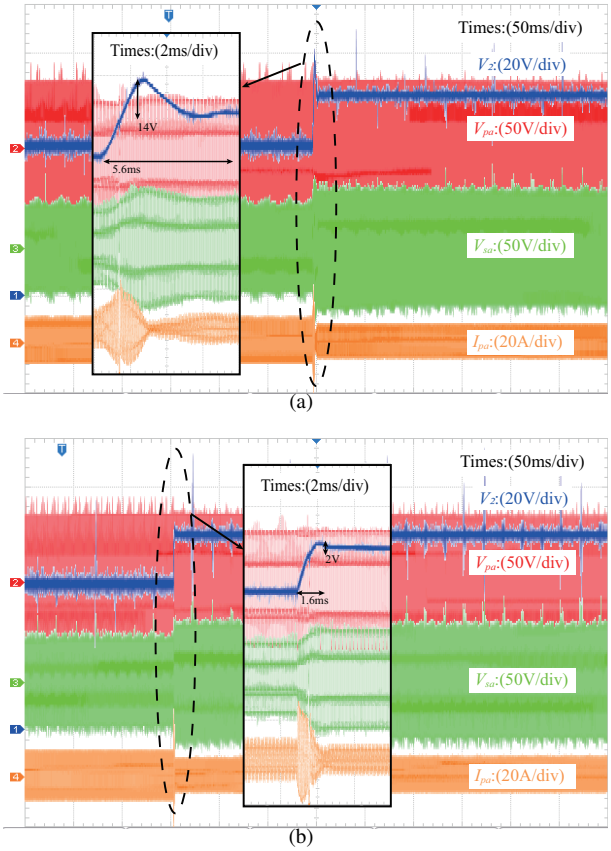

Fig. 10. Related waveforms of 3p-DAB for the step change of the reference output voltage. (a) PI control based on PSM. (b) Proposed control scheme.

The experiment comparison of the step change of the reference output voltage are conducted in this section. The voltage voltage reference is varied from 60V to 80V, and the load resistor is maintain as 20Ω. The comparison results are shown in Fig. 10. It can be found that the transition time is

decreased from 5.6ms by PI control based on PS modulation to 1.6ms by the proposed control strategy, and the overshoot voltage is reduced from 14V by PI control based on PSM to 2V by the proposed control strategy. The above experimental comparison result further verifies the theoretic analysis and the effectiveness of the proposed control scheme.

V. Conclusion

In this paper, a novel nonlinear controller combined with the PD controller and the Adaline is proposed to improve the dynamic performance of the 3p-DAB. Firstly, an SMLA is presented to renew the weighting vector of the Adaline for enhancing the robustness of adaptive learning. Meanwhile, the output of the Adaline is added to the output of a PD controller to maintain an excellent dynamic performance for output voltage regulation. Then, the comparison simulation results are shown to validate the theoretic analysis and the effectiveness of the proposed control scheme. Finally, the experimental comparison results on a laboratory prototype are provided to further verify the effectiveness and superiority of the proposed control strategy.

Acknowledgment

This work was supported in part by National Key R&D Program of China (2018YFB1201804), in part by the National Natural Science Foundation of China under Grants 51807177, 51827810, 51637009, 51977193, in part by China Postdoctoral Science Foundation under Grant 2020M681855, and in part by Natural Science Foundation of Zhejiang Province under Grant LY21E070004.

References

[1] Q. Xu, N. Vafamand, L. Chen, T. Dragičević, L. Xie, and F. Blaabjerg, "Review on advanced control technologies for bidirectional DC/DC converters in DC microgrids," *IEEE J. Emerg. Sel. Topics Power Electron.*, vol. 9, no. 2, pp. 1205-1221, Apr. 2021.

[2] L. Chen, F. Gao, K. Shen, Z. Wang, L. Tarisciotti, P. Wheeler, and T. Dragičević, "Predictive control based DC microgrid stabilization with the dual active bridge converter," *IEEE Trans. Ind. Electron.*, vol. 67, no. 10, pp. 8944-8956, Oct. 2020.

[3] H. Shi, H. Wen, J. Chen, Y. Hu, L. Jiang, and G. Chen, "Minimum-reactive-power scheme of dual-active-bridge DC-DC converter with three-level modulated phase-shift control," *IEEE Trans. Ind. Appl.*, vol. 53, no. 6, pp. 5573-5586, Dec. 2017.

[4] J. Hu, S. Cui, D. v. d. Hoff, and R. W. De Doncker, "Generic dynamic phase-shift control for bidirectional dual-active bridge converters," *IEEE Trans. Power Electron.*, vol. 36, no. 6, pp. 6197-6202, Jun. 2021.

[5] S. Shao, M. Jiang, W. Ye, Y. Li, J. Zhang, and K. Sheng, "Optimal Phase-Shift Control to Minimize Reactive Power for a Dual Active Bridge DC-DC Converter," *IEEE Trans. Power Electron.*, vol. 34, no. 10, pp. 10193-10205, Oct. 2019.

[6] J. Sun, L. Qiu, X. Liu, J. Zhang, J. Ma, and Y. Fang, "Optimal simultaneous PWM control for three-phase dual-active-bridge converters to minimize current stress in the whole load range," *IEEE J. Emerg. Sel. Topics Power Electron.*, DOI: 10.1109/JESTPE.2020.3047400.

[7] J. Sun, L. Qiu, X. Liu, J. Ma, and Y. Fang, "Modified Model Predictive Control for Three-Phase Dual-Active-Bridge DC-DC Converters with Recursive Least Square Estimation," *2021 IEEE Energy Conversion Congress and Exposition - Asia (ECCE- Asia), Singapore*, 2021, pp. 720-725.

[8] H. Qin and J. W. Kimball, "Closed-loop control of DC-DC dual-active-bridge converters driving single-phase inverters," *IEEE Trans. Power Electron.*, vol. 29, no. 2, pp. 1006-1017, Feb. 2014.

[9] D. Segaran, D. G. Holmes, and B. P. McGrath, "Enhanced load step response for a bidirectional DC-DC converter," *IEEE Trans. Power Electron.*, vol. 28, no. 1, pp. 371-379, Jan. 2013.

[10] W. Zhao, X. Zhang, S. Gao, and M. Ma, "Improved model-based phase-shift control for fast dynamic response of dual-active-bridge DC/DC converters," *IEEE J. Emerg. Sel. Topics Power Electron.*, vol. 9, no. 1, pp. 223-231, Feb. 2021.

[11] S. P. Engel, N. Soltau, H. Stagge, and R. W. De Doncker, "Improved instantaneous current control for the three-phase dual-active bridge DC-DC converter,"*2013 IEEE Energy Conversion Congress and Exposition - Asia (ECCE- Asia), Melbourne*, 2013, pp. 855-860.

[12] S. P. Engel, N. Soltau, H. Stagge and R. W. De Doncker, "Improved instantaneous current control for high-power three-phase dual-active bridge DC-DC converters," *IEEE Trans. Power Electron.*, vol. 29, no. 8, pp. 4067-4077, Aug. 2014.

[13] J. Huang, Z. Li, L. Shi, Y. Wang, and J. Zhu, "Optimized modulation and dynamic control of a three-phase dual active bridge converter with variable duty cycles," *IEEE Trans. Power. Electron.*, vol. 34, no. 3, pp. 2856-2873, Mar. 2019.

[14] N. Soltau, H. A. B. Siddique and R. W. De Doncker, "Comprehensive modeling and control strategies for a three-phase dual-active bridge," *2012 International Conference on Renewable Energy Research and Applications (ICRERA), Nagasaki, Japan*, 2012, pp. 1-6.

[15] K. Johan and T. Hägglund, *Advanced PID Control*, Pittsburgh, PA, USA: Instrum., Syst., Autom. Soc., 2006.